Risk score model of autophagy-related genes in osteosarcoma

Wentao Qin
Guangxi Medical University First Affiliated Hospital
Mingyang Jiang
Guangxi Medical University First Affiliated Hospital
Yang Hu
Guangxi Medical University First Affiliated Hospital
Mingjing Xie
Guangxi Medical University First Affiliated Hospital
Yiji Jike
Guangxi Medical University First Affiliated Hospital
Zhandong Bo (drrbozhandong@126.com)
Guangxi Medical University First Affiliated Hospital https://orcid.org/0000-0001-6827-4508

Research article

Keywords: autophagy gene, osteosarcoma, risk prediction model

Posted Date: September 30th, 2021

DOI: https://doi.org/10.21203/rs.3.rs-936589/v1

Abstract

Background

Osteosarcoma (OS) is the most common primary malignancy in children and adolescents, with a high mortality and disability rate. Autophagy plays an important role in the regulation of apoptosis, invasion and metastasis of tumor cells. Hence, construction of a risk score model of autophagy related genes (ARGs) of OS would benefit the treatment and prognosis evaluation.

Methods

We downloaded a dataset of OS from The Cancer Genome Atlas (TCGA) database, and found the OS-related ARGs through Human Autophagy Database (HADb). Five hub ARGs (CCL2, AMBRA1, VEGFA, MYC and EGFR) were obtained by using multivariate Cox regression model. Then we calculated the risk scores and constructed a prediction model. Another two datasets downloaded from GEO were combined to verify the accuracy and validity of the model. The role of immune cell infiltration was systematically explored, and prediction of response to targeted drugs was assessed. Immunohistochemistry was carried out to verify the expression of the key ARGs.

Results

Based on these five hub ARGs, we constructed a risk score model related to OS. High accuracy and validity were demonstrated by datasets downloaded from GEO. These five ARGs played a role in cancer-related biological processes, such as MAPK pathway and PI3K pathway. The results of targeted drug sensitivity analyses coincided with the pathway analysis. Immunohistochemistry showed that the expression of 5 ARGs in OS group was more obvious than that in paracancerous group.

Conclusion

This study constructs a risk score model related to autophagy of OS, explores the prognostic value of autophagy related genes, and finds possible therapeutic targets.

Introduction

Osteosarcoma (OS) is the most common primary malignancy in children and adolescents, with a high mortality and disability rate (1). With the deepening understanding of tumor pathogenesis and the development of diagnosis and treatment techniques, the 5-year survival rate of patients with OS has increased from less than 20–50%-60% (2). As a way for cells to survive in abnormal environments, autophagy plays an important role in the regulation of apoptosis, invasion and metastasis of tumor cells

(3). Hence, construction of a risk score model of autophagy related genes (ARGs) of OS would benefit the treatment and prognosis evaluation.

The Cancer Genome Atlas (TCGA) uses high-throughput genome sequencing, gene chip technology and multi-dimensional data integration analysis method to map out the genome variation and gene expression level of almost all human cancers (4). It will eventually clarify the occurrence and development mechanism of cancer, and develop new diagnosis, classification standards and treatment methods on this basis.

In order to predict the occurrence of OS through autophagy, we downloaded a gene expression microarray dataset from TCGA, and select autophagy related genes. After normalization, we performed a multiple COX regression model along with 10-fold cross validation to construct a prediction score model (5). Another two datasets from Gene Expression Omnibus (GEO) was used to verify the accuracy and validity (6). Finally, we collected 10 samples from Guangxi Medical University First Affiliated Hospital to further validate the expression of the five ARGs through immunohistochemistry.

Methods

Data preparation

The gene expression profiles and clinical information of osteosarcoma patients (TARGET-OS) was downloaded as training set from the TCGA database (https://www.cancer.gov/about-nci/organization/ccg/research/structural-genomics/tcga) (7, 8). Clinical information including survival time, survival state, gender, age, disease at diagnosis, primary tumor site, specific tumor region and definitive surgery. The autophagy information used for selecting autophagy relative genes (ARGs) was downloaded from Human Autophagy Database (HADb) (http://www.autophagy.lu/index.html) (9). In order to verify the accuracy of risk model and nomogram prediction, two datasets (GSE16091, GSE39058) were downloaded as validation set from the GEO database (https://www.ncbi.nlm.nih.gov/geo). Since the two datasets come from different platforms, we first use the normalizeBetweenArrays function to correct the datasets, then merge the two datasets and use "ComBat" package of R to perform batch corrections between the datasets.

Construction of autophagy prediction of risk score model

Univariate Cox regression analysis was conducted for OS related ARGs, and the clinical factor was taken into consideration. Then, a multivariate Cox regression analysis model along with the LASSO method for variable selection and shrinkage was applied to build a autophagy prediction of risk model by using the GLMNET package (https://CRAN.R-project.org/package=glmnet) (5). The penalty regularization parameter k was determined via the cross-validation routine cv. glmnet before running the main algorithm with an n-fold value equal to 10. The k value was finalized by using lambda. min, which is the value of lambda giving minimum mean cross-validated error (10, 11). Genes with corresponding efficiencies were screened from the TARGET-OS training set and used to construct a risk score model for autophagy

prediction. According to the model, the risk score of each person was calculated. The algorithm of the risk score was as follows: $\sum nx=1(coefx \times Exprx)$ in which coefx was the regression coefficient of key ARGs in patient x obtained by multivariate Cox proportional risk regression analysis, and Exprx represents the expression level of one of the key ARGs in patient x (12). Patients were assigned to high- and low- risk groups according to the median of risk scores. Then, we used the "Survival" package of R to draw a Kaplan–Meier survival curve. In order to avoid the mutual influence between risk factors, we carried out principal component analysis (PCA) and performed dimensionality reduction. According to several key ARGs and risk scores in the risk model, we drew a nomogram with R's "Reglot" package to predict the 1-, 3- and 5-year survival rates of OS patients. The scale on the nomogram line represents the range of values for each variable, and the total score calculated for each variable could be used to predict survival (13).

Validation of the risk score model

We used the receiver operating characteristic curve (ROC) drawn by " Survival ROC" package and the calibration curve obtained by "RMS" package to evaluate the accuracy of their prediction of 1-, 3- and 5-year survival rates, and used ROC curve to verify each grouping variable (14). In addition, diagnostic value of key ARGs were validated by a dataset from GEO databases, and the diagnostic value of each key ARGs was evaluated by AUC.

Gene enrichment analysis (GO and KEGG)

We investigate molecular function (MF), biological process (BP) and cellular components (CC) of the ARGs in GO database. And selected ARGs were utilized in the functional pathway analysis of KEGG. R software and ClusterProfiler package were used to conduct the results of functional enrichment analysis. The correlation between ARGs was analyzed by Pearson's correlation coefficient using the corrplot package.

Gene set enrichment analysis (GSEA)

GSEA analysis was performed to identify the potential function of selected hub genes. Genome-wide expression profile datasets and corresponding grouping files determined by the expression of ARGs were uploaded to GSEA4.0.3 software (15) for enrichment analysis with database C2 and C5 of the Molecular Signatures Database (MSigDB) (16). A set of genes with |normal enrichment score| (|NES|)>1, false discovery rate (FDR) <0.25 and P<0.05 was considered to be statistically significant.

Immune infiltrating

The proportion of the 29 immune signatures was quantified (16 immune cell and 13 immune-associated function signatures) in each OS sample. The ESTIMATE algorithm was applied to evaluate the immune cell infiltration level (immune score) and the stromal content (stromal score) for each OS sample. The ConsensuClusterPlus R package was used to perform consensus clustering of each OS sample based on the 29 immune signature.

Prediction of response to targeted therapy drugs

Half maximal inhibitory concentration (IC50) of common targeted therapy drugs was calculated to evaluate clinical responses to OS treatment using pRRophetic [13] and ggplot2 packages in R. The relationship between IC50s and high- and low-risk groups was represented by box plots.

Immunohistochemistry

We obtained 5 OS and 5 paracancerous samples from Guangxi Medical University First Affiliated Hospital for immunohistochemistry. All patients were diagnosed as OS by pathology. The clinicopathological data, such as gender and age were collected.

The tissue slices were placed in xylene for 20min, then replaced with fresh xylene and repeated once. The dewaxed tissue slice was soaked in 100% ethanol for 5min twice, 95% ethanol, 80% ethanol and distilled water for 5min respectively. The alkaline antigen repair solution (Tri-EDTA, pH=9) was heated to the boil in a pressure cooker, the tissue slice was placed in, and the time was timed for 2 min, then cooled to room temperature naturally (17). Incubate with 3% H_2O_2 at room temperature for 10 min in dark, and then block with normal sheep serum solution at room temperature for 30min. The primary antibody RP215 was added at 4℃ overnight and HRP-labeled secondary antibody was treated at room temperature for 30min. DAB color, hematoxylin redyeing (17).

Ten high-power (400×) visual fields were randomly selected, and two researchers independently read the images. The nucleus of hematoxylin stained is blue, and the positive expression of DAB is brownish yellow.

Statistical analysis.

All data were statistically analyzed using SPSS22.0(IBM) and R 3.6.2 (https://www.r project.org/). Risk ratio (HR) and 95% confidence interval (CI) were used to represent the relative risk between each variable and the prognosis of OS patients. All results $P < 0.05$ were considered statistically significant (6).

Results

Analysis and collation of ARGs data.

Expression files of 85 patients (from TARGET-OS, all diagnosed with osteosarcoma) were downloaded from TCGA and 232 autophagy genes on HADb were combined to find OS related ARGs and their expression level and clinical information. Expression files of 81 patients (34 from GSE16091, 47 from GSE39058, all diagnosed with osteosarcoma) from GEO were downloaded to verify the stability of the model. After univariate Cox analysis, 10 survival related ARGs were obtained (Figure 1A). Based on the expression profile, we used a multivariate Cox regression along with the LASSO method to build a classifier to predict OS (Figure 1B-C). A combination of 5 genes (CCL2, AMBRA1, VEGFA, MYC and EGFR) was selected as the best predictor of OS in the training cohort (Figure 1D).

Data preprocessing and risk score model construction

Patients in the training and validation sets were assigned to high- and low-risk groups using the median risk score of the training set. Survival analysis between the high- and low- risk score groups indicated that a high-risk score was significantly associated with the poor outcome of patients with OS (Figure 2A-B). The expression level of 5 genes from the signature was plotted as a heatmap (Figure 2C). Similar results were observed in the validation set (Figure 2D-F). According to the results, the expression levels of CCL2, AMBRA1 and EGFR were relatively lower in patients with autophagy. On the contrary, patients with autophagy tended to have a higher expression level of VEGFA and MYC. The survival rates and gene expression levels of each hub ARG were displayed (Figure 3).

Nomogram development and verification

The gene expression profiles and clinical information of TARGET-OS were mined previously. After PCA, risk score combined with 5 independently related risk factors (gender, age, disease at diagnosis, definitive surgery and risk score) were used to form a OS risk estimation nomogram (Figure 4). Kaplan–Meier curve showed that with time growing, the survival rate of the high-risk group is lower than that of the low-risk group, and the difference is statistically significant (Figure 5A). The C-index (0.853 in training set) and calibration curve were plotted to evaluate prediction accuracy (Figure 5B-C). The C-index (0.879 in validation set) and calibration curve in the validation set also revealed consistent predicted and actual survival rates (Figure 5D-F). High accuracy was demonstrated in these two datasets, indicating the stability of the risk score model.

KEGG and GO functional enrichment analysis

To clarify the biological pathways and processes related to the 5 ARGs, GO biological process enrichment and KEGG signaling pathway analysis were carried out. The results indicated that these 5 ARGs play an important role in autophagy-related processes such as MAPK signaling pathway and PI3K-Akt signaling pathway (Figure 6).

GSEA

The patients were stratified according to the median of risk scores, and GSEA results revealed that the five ARGs were favorably enriched in biocarta-TOB1 pathway, antigen receptor mediate signaling pathway, inflammatory response to antigenic stimulus, membrane invagination, phagocytic vesicle membrane, regulation of lymphocyte activation, T cell receptor signaling pathway, NK cell mediated cytotoxicity, reactome costimulation by the CD28 family and reactome signaling by the B cell receptor, which were displayed (Figure 7).

Immune infiltrating

The immune cell infiltration level was further evaluated, as well as the immune function level of the two groups. We found that low-risk group was marked by all immune cell and immune function infiltration,

except aDCs and iDCs. On the contrary, the subject in high-risk group almost all had low immune cell and immune function infiltration (Figure 8A-B). A heat map was generated to show the distribution of various immune cells in osteosarcoma tissues of patients in the five groups (Figure 8C).

Response to targeted therapy drugs

According to the predicted IC50s, the high- and low- risk groups had different responses to various targeted drugs, and the difference was statistically significant. The high-risk group had lower IC50s, which indicated that the high-risk group was more sensitive to targeted drugs (Figure 9).

Immunohistochemistry

The expressions of 5 hub genes in OS group were more obvious than that in paracancerous group (Figure 10).

Discussion

Nowadays, more and more studies show that autophagy plays an important role in the development and treatment of OS. Autophagy is a "self-digestion" metabolic process of cell renewal, which has been proved to continue the growth of tumor cells by maintaining cell energy production (18). In addition, inhibition of autophagy has also been proved to enhance the effectiveness of anti-cancer therapy (19). These evidences will bring the hope of molecular targeted therapy to OS patients.

In this study, we screened OS-related ARGs to obtain 5 key ARGs, which are potential targets for new molecular targeted therapies. A risk prediction model was constructed for these five key ARGs, and it was found that the survival curves of the low-risk group and the high-risk group were significantly separated (17). In the time-dependent model, the risk score and the number of deaths increased significantly with the time, indicating that these five key ARGs are of great significance in predicting OS prognosis. From the ROC prediction results of 1-, 3-, and 5-year survival rates, 5 key ARGs could predict the prognosis of OS patients well. Similarly, five key ARGs also showed satisfactory results in the study of clinical traits.

Four of the five key ARGs have been experimentally proved and reported to be related to OS. Monocyte chemotactic protein-1 (MCP-1/CCL2) is an important immune factor, which may be important in cancer progression by promoting proliferation, invasion, metastasis and the tumor microenvironment. Previous studies have identified that the expression of CCL2 is high in high-grade osteosarcoma cells and promotes the proliferation and invasion of osteosarcoma cells (20). Another study found that MicroRNA-150-5p weakens proliferative and invasive potentials in osteosarcoma cells by downregulating VEGFA level. And the knockdown of VEGFA remarkably weakened osteosarcoma cell proliferative and invasive capacities (21). Moreover, a few researchers applied multi-region whole-genome sequencing to identify that amplification of the MYC oncogene is a major driver of childhood osteosarcoma (22). And previous research uncovered an important role of the /miR-7/EGFR pathway in the migration and invasion of osteosarcoma cells and suggested that may be a prognostic marker and a promising therapeutic target

for osteosarcoma (23). As for now, AMBRA1 has not been found to be directly related to OS, but it was identified that AMBRA1 was related to the occurrence and progression of many tumors, such as, rectal cancer and prostatic cancer.

According to the results of enrichment analyses, autophagy of OS is closely related to MAPK signaling pathway and PI3K – Akt signaling pathway. Precious studies demonstrated that PEITC induced autophagy in K7M2 osteosarcoma cells by activating the ROS-related MAPK signaling pathway (24); escin counteracted osteosarcoma by inducing autophagy and apoptosis via the activation of the ROS/p38 MAPK signaling pathway (25). Jin et al. found that miR-1224-5p targeted PLK1 to inhibit PI3K/Akt/mTOR signaling pathway, thus mediating the autophagy (26). These studies verified that our results were credible. GSEA suggests that autophagy of OS is favorably related to immune and inflammatory response. Related pathways including T cells, B cells and NK cells may be the potential direction of targeted therapy.

The model suggested that high-risk scores were associated with sensitivity to targeted drugs. Previous studies have demonstrated the role of these drugs in cancer biological cytology. For example, Axitinib (AG-013736) is a potent and selective inhibitor of VEGFR 1–3. In transfected or endogenous RTK-expressing cells, Axitinib potently blocks growth factor-stimulated phosphorylation of VEGFR-2 and VEGFR-3 (27, 28). AZD8055 showed low activity against all PI3K subtypes (α, β, γ, δ) and other near-PI3K kinase families (ATM and DNA-PK). AZD8055 inhibits the phosphorylation of mTORC1(p70S6K and 4E-BP1), mTORC2 (AKT), and downstream proteins (29). BIRB 796 is one of the most effective and slowest-separating inhibitors of human p38 MAPK (30). Combination of BIRB0796 with p38 MAPKs or JNK1/2 decreased phosphorylation of upstream kinase MKK6 or MKK4, but did not enhance dephosphorylation (31). The results of these drug sensitivity analyses coincided with the results of the above-mentioned pathway analysis.

Tumor-associated immune response plays an important role in cell infiltration in tumor microenvironment, whereas autophagy plays a key regulatory role in tumor-related immune responses (32). Immune infiltration analyses revealed that the immune response and immune system processes were significantly enriched in the low-risk group, suggesting that low-risk patients have autophagy-related, anti-tumor immune response processes that reduce the risk of death.

However, there were some limitations remain to be solved. 1. The number of patients in the dataset is not sufficient. Additional patients should be involved and more sufficient clinical information should be collected to further verify the stability of the model. 2. Some possible ARGs may be excluded due to our stringent inclusion criteria. 3. Functional annotation analysis was performed on the target gene based on bioinformatics analysis. More experiments are required to validate and even correct the KEGG pathway analysis and GO enrichment results.

Conclusion

We constructed a risk score model based on five ARGs related to OS and verified the accuracy and stability. Functional enrichment analyses indicated that the genes in the risk scores were involved in several classical cancer-related biological processes. The role of immune cell infiltration was systematically explored, and prediction of response to targeted drugs was assessed. Immunohistochemistry demonstrated that the five hub ARGs obviously expressed in OS tissue slices. This risk score model provides the basis for the prediction of OS autophagy and the potential guidance for the treatment.

Declarations

Ethics approval and consent to participate

This study was approved by Guangxi Medical University First Affiliated Hospital ethical review committee, approval number:2021(KY-E-125)

Consent for publication

All authors agreed to publish the study.

Availability of data and material

None.

Competing interests

None.

Funding

2017JJA10088

Authors' contributions

W.Q. and M.J. designed the study

Y.H., M.X. and Y.J. collected the samples and implemented experiment.

Z.B. finally approved the manuscript

Acknowledgments

The authors thank he Guangxi Medical University First Affiliated Hospital for the assistance offered in the data collection.

References

1. Pingping B, Yuhong Z, Weiqi L, Chunxiao W, Chunfang W, Yuanjue S, Chenping Z, Jianru X, Jiade L, Lin K, et al. Incidence and mortality of sarcomas in shanghai, china, during 2002–2014. FRONT ONCOL. 2019;9:662. doi:10.3389/fonc.2019.00662.
2. Sayles LC, Breese MR, Koehne AL, Leung SG, Lee AG, Liu HY, Spillinger A, Shah AT, Tanasa B, Straessler K, et al. Genome-informed targeted therapy for osteosarcoma. CANCER DISCOV. 2019;9(1):46–63. doi:10.1158/2159-8290.CD-17-1152.
3. Jin B, Jin D, Zhuo Z, Zhang B, Chen K. Mir-1224-5p activates autophagy, cell invasion and inhibits epithelial-to-mesenchymal transition in osteosarcoma cells by directly targeting plk1 through pi3k/akt/mtor signaling pathway. Onco Targets Ther. 2020;13:11807–18. doi:10.2147/OTT.S274451.
4. Wang L, Xie Y, Fang H, Zhang X, Pan H, Yan S. Long noncoding rna dancr in various cancers: a meta-analysis and bioinformatics. CANCER MANAG RES. 2019;11:6581–92. doi:10.2147/CMAR.S200922.
5. Dong S, Huo H, Mao Y, Li X, Dong L. A risk score model for the prediction of osteosarcoma metastasis. FEBS OPEN BIO. 2019;9(3):519–26. doi:10.1002/2211-5463.12592.
6. Zhong X, Liu Y, Liu H, Zhang Y, Wang L, Zhang H. Identification of potential prognostic genes for neuroblastoma. FRONT GENET. 2018;9:589. doi:10.3389/fgene.2018.00589.
7. Liu X, Hu AX, Zhao JL, Chen FL. Identification of key gene modules in human osteosarcoma by co-expression analysis weighted gene co-expression network analysis (wgcna). J CELL BIOCHEM. 2017;118(11):3953–9. doi:10.1002/jcb.26050.
8. Zhang J, Lan Q, Lin J. Identification of key gene modules for human osteosarcoma by co-expression analysis. WORLD J SURG ONCOL. 2018;16(1):89. doi:10.1186/s12957-018-1381-y.
9. Homma K, Suzuki K, Sugawara H. The autophagy database: an all-inclusive information resource on autophagy that provides nourishment for research. *NUCLEIC ACIDS RES* (2011) 39(Database issue):D986-D990. doi: 10.1093/nar/gkq995.
10. Birnbaum DJ, Finetti P, Lopresti A, Gilabert M, Poizat F, Raoul JL, Delpero JR, Moutardier V, Birnbaum D, Mamessier E, et al. A 25-gene classifier predicts overall survival in resectable pancreatic cancer. BMC MED. 2017;15(1):170. doi:10.1186/s12916-017-0936-z.
11. Mao Y, Fu Z, Zhang Y, Dong L, Zhang Y, Zhang Q, Li X, Wang C. A six-microrna risk score model predicts prognosis in esophageal squamous cell carcinoma. J CELL PHYSIOL. 2019;234(5):6810–9. doi:10.1002/jcp.27429.
12. Han B, Zhang H, Zhu Y, Han X, Wang Z, Gao Z, Yuan Y, Tian R, Zhang F, Niu R. Subtype-specific risk models for accurately predicting the prognosis of breast cancer using differentially expressed autophagy-related genes. Aging. 2020;12(13):13318–37. doi:10.18632/aging.103437.
13. Liao S, He J, Liu C, Zhang Z, Liao H, Liao Z, Yu C, Guan J, Mo H, Yuan Z, et al. Construction of autophagy prognostic signature and analysis of prospective molecular mechanisms in skin cutaneous melanoma patients. Med (Baltim). 2021;100(22):e26219. doi:10.1097/MD.0000000000026219.

14. Jiao Y, Fu Z, Li Y, Meng L, Liu Y. High eif2b5 mrna expression and its prognostic significance in liver cancer: a study based on the tcga and geo database. CANCER MANAG RES. 2018;10:6003–14. doi:10.2147/CMAR.S185459.
15. Subramanian A, Tamayo P, Mootha VK, Mukherjee S, Ebert BL, Gillette MA, Paulovich A, Pomeroy SL, Golub TR, Lander ES, et al. Gene set enrichment analysis: a knowledge-based approach for interpreting genome-wide expression profiles. Proc Natl Acad Sci U S A. 2005;102(43):15545–50. doi:10.1073/pnas.0506580102.
16. Liberzon A, Birger C, Thorvaldsdottir H, Ghandi M, Mesirov JP, Tamayo P. The molecular signatures database (msigdb) hallmark gene set collection. CELL SYST. 2015;1(6):417–25. doi:10.1016/j.cels.2015.12.004.
17. Xu J, Nie H, He J, Wang X, Liao K, Tu L, Xiong Z. Using machine learning modeling to explore new immune-related prognostic markers in non-small cell lung cancer. FRONT ONCOL. 2020;10:550002. doi:10.3389/fonc.2020.550002.
18. Choi AM, Ryter SW, Levine B. Autophagy in human health and disease. N Engl J Med. 2013;368(7):651–62. doi:10.1056/NEJMra1205406.
19. Giampieri F, Afrin S, Forbes-Hernandez TY, Gasparrini M, Cianciosi D, Reboredo-Rodriguez P, Varela-Lopez A, Quiles JL, Battino M. Autophagy in human health and disease: novel therapeutic opportunities. Antioxid Redox Signal. 2019;30(4):577–634. doi:10.1089/ars.2017.7234.
20. Chen Q, Sun W, Liao Y, Zeng H, Shan L, Yin F, Wang Z, Zhou Z, Hua Y, Cai Z. Monocyte chemotactic protein-1 promotes the proliferation and invasion of osteosarcoma cells and upregulates the expression of akt. MOL MED REP. 2015;12(1):219–25. doi:10.3892/mmr.2015.3375.
21. Qin Y, Zhang B, Ge BJ. Microrna-150-5p inhibits proliferation and invasion of osteosarcoma cells by down-regulating vegfa. Eur Rev Med Pharmacol Sci. 2020;24(18):9265–73. doi:10.26355/eurrev_202009_23008.
22. De Noon S, Ijaz J, Coorens TH, Amary F, Ye H, Strobl A, Lyskjaer I, Flanagan AM, Behjati S. Myc amplifications are common events in childhood osteosarcoma. J Pathol Clin Res. 2021. doi:10.1002/cjp2.219.
23. Li H, Lan M, Liao X, Tang Z, Yang C. Circular rna cir-itch promotes osteosarcoma migration and invasion through cir-itch/mir-7/egfr pathway. Technol Cancer Res Treat. 2020;19:1078166376. doi:10.1177/1533033819898728.
24. Lv HH, Zhen CX, Liu JY, Shang P. Peitc triggers multiple forms of cell death by gsh-iron-ros regulation in k7m2 murine osteosarcoma cells. ACTA PHARMACOL SIN. 2020;41(8):1119–32. doi:10.1038/s41401-020-0376-8.
25. Zhu J, Yu W, Liu B, Wang Y, Shao J, Wang J, Xia K, Liang C, Fang W, Zhou C, et al. Escin induces caspase-dependent apoptosis and autophagy through the ros/p38 mapk signalling pathway in human osteosarcoma cells in vitro and in vivo. CELL DEATH DIS. 2017;8(10):e3113. doi:10.1038/cddis.2017.488.

26. Jin B, Jin D, Zhuo Z, Zhang B, Chen K. Mir-1224-5p activates autophagy, cell invasion and inhibits epithelial-to-mesenchymal transition in osteosarcoma cells by directly targeting plk1 through pi3k/akt/mtor signaling pathway. Onco Targets Ther. 2020;13:11807–18. doi:10.2147/OTT.S274451.
27. Hu-Lowe DD, Zou HY, Grazzini ML, Hallin ME, Wickman GR, Amundson K, Chen JH, Rewolinski DA, Yamazaki S, Wu EY, et al. Nonclinical antiangiogenesis and antitumor activities of axitinib (ag-013736), an oral, potent, and selective inhibitor of vascular endothelial growth factor receptor tyrosine kinases 1, 2, 3. CLIN CANCER RES. 2008;14(22):7272–83. doi:10.1158/1078-0432.CCR-08-0652.
28. Fenton BM, Paoni SF. The addition of ag-013736 to fractionated radiation improves tumor response without functionally normalizing the tumor vasculature. CANCER RES. 2007;67(20):9921–8. doi:10.1158/0008-5472.CAN-07-1066.
29. Chresta CM, Davies BR, Hickson I, Harding T, Cosulich S, Critchlow SE, Vincent JP, Ellston R, Jones D, Sini P, et al. Azd8055 is a potent, selective, and orally bioavailable atp-competitive mammalian target of rapamycin kinase inhibitor with in vitro and in vivo antitumor activity. CANCER RES. 2010;70(1):288–98. doi:10.1158/0008-5472.CAN-09-1751.
30. Pargellis C, Tong L, Churchill L, Cirillo PF, Gilmore T, Graham AG, Grob PM, Hickey ER, Moss N, Pav S, et al. Inhibition of p38 map kinase by utilizing a novel allosteric binding site. Nat Struct Biol. 2002;9(4):268–72. doi:10.1038/nsb770.
31. Kuma Y, Sabio G, Bain J, Shpiro N, Marquez R, Cuenda A. Birb796 inhibits all p38 mapk isoforms in vitro and in vivo. J BIOL CHEM. 2005;280(20):19472–9. doi:10.1074/jbc.M414221200.
32. Marar C, Starich B, Wirtz D. Extracellular vesicles in immunomodulation and tumor progression. NAT IMMUNOL. 2021;22(5):560–70. doi:10.1038/s41590-021-00899-0.

Figures

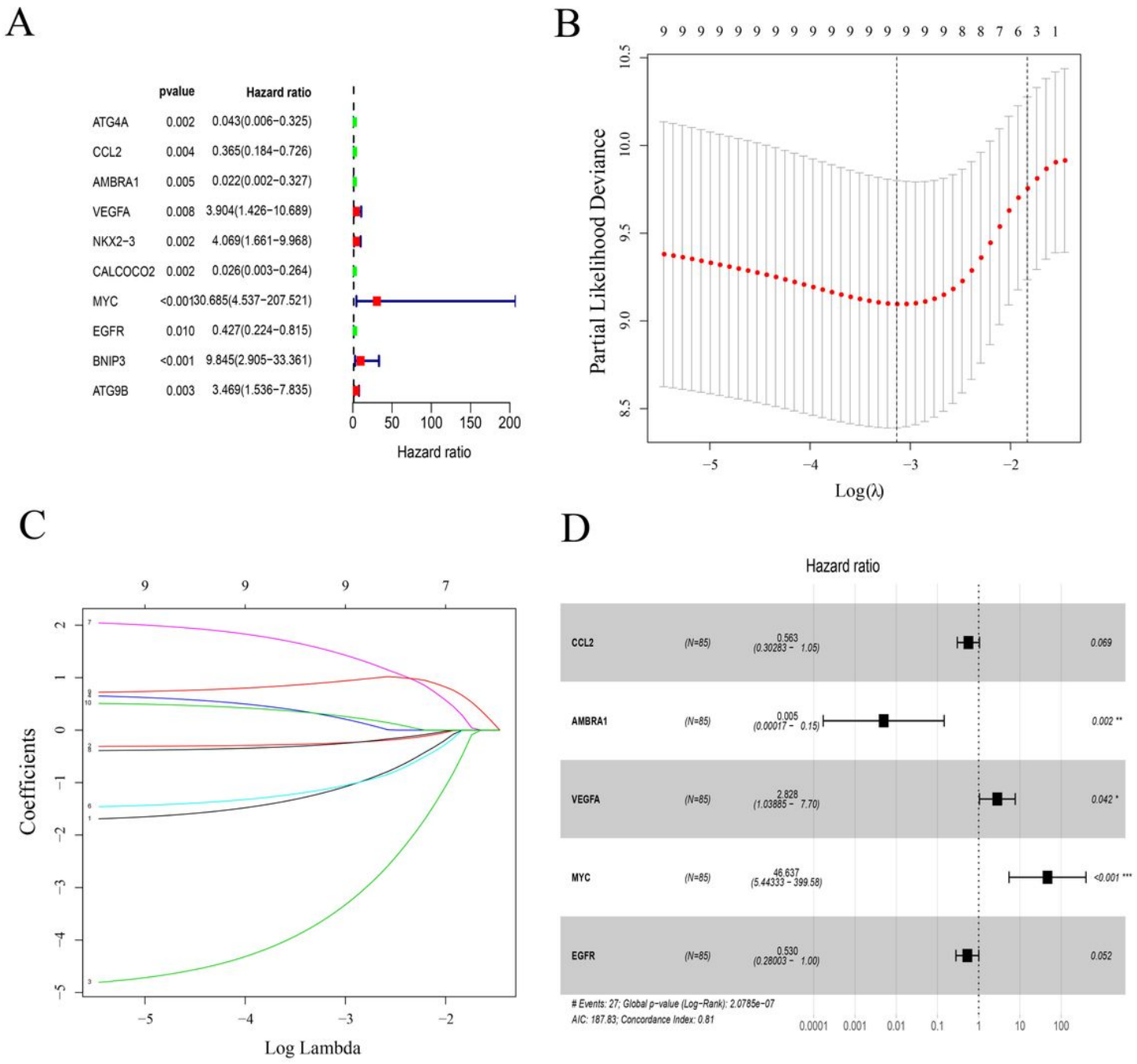

Figure 1

(A) Forrest plot of univariate Cox regression. (B) Risk score model construction using LASSO logistic regression analysis along with 10-fold cross validation. Partial likelihood deviance was plotted versus log(Lambda). The vertical dotted line indicates the lambda value with the minimum error and the largest lambda value where the deviance is within one SE of the minimum. (C) LASSO coefficient profiles of the genes associated with the metastasis of osteosarcoma. (D) Forrest plot of multivariate Cox regression.

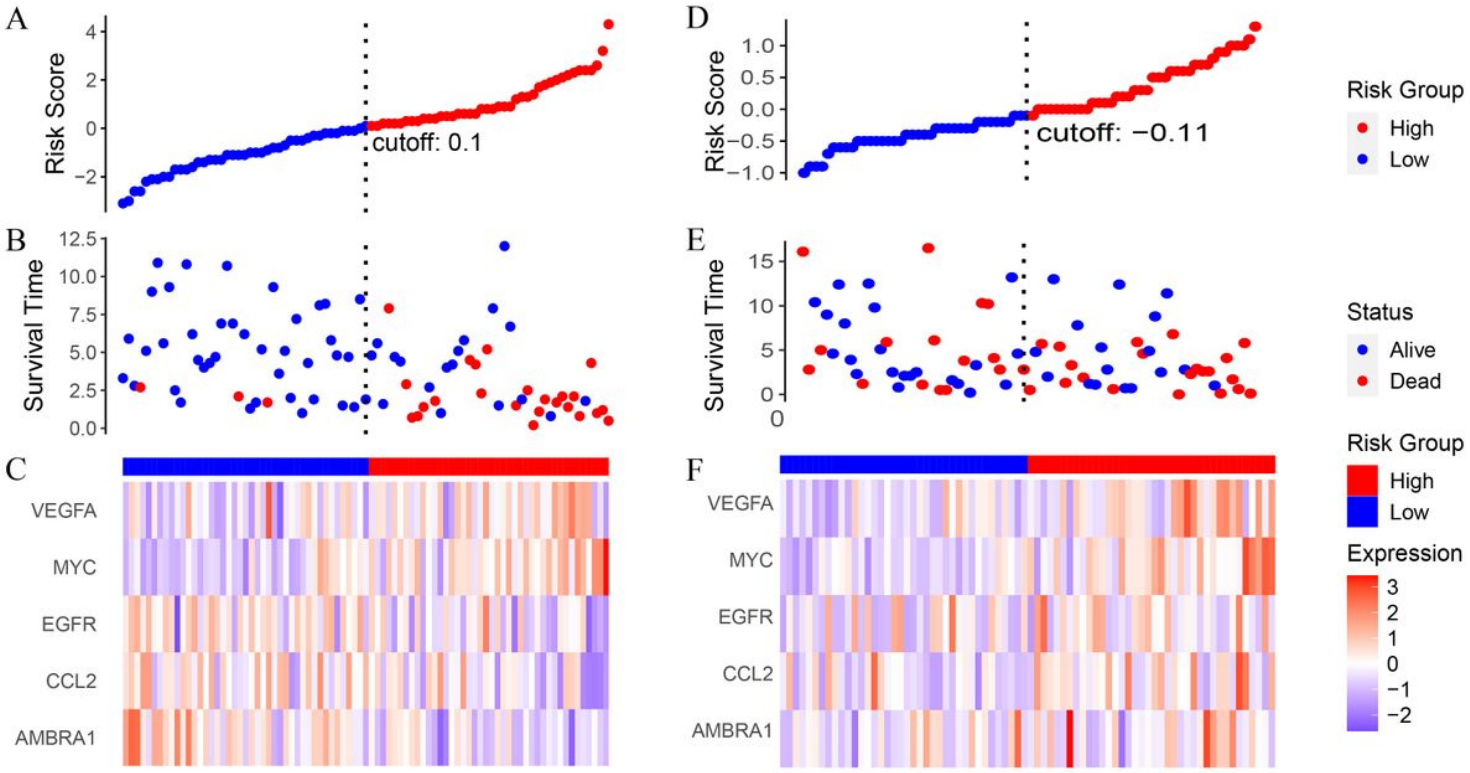

Figure 2

(A) Risk score plot (B) survival status scatter plot and (C) heat map of the expression levels of CCL2, AMBRA1, VEGFA, MYC and EGFR in low-and high-risk groups.

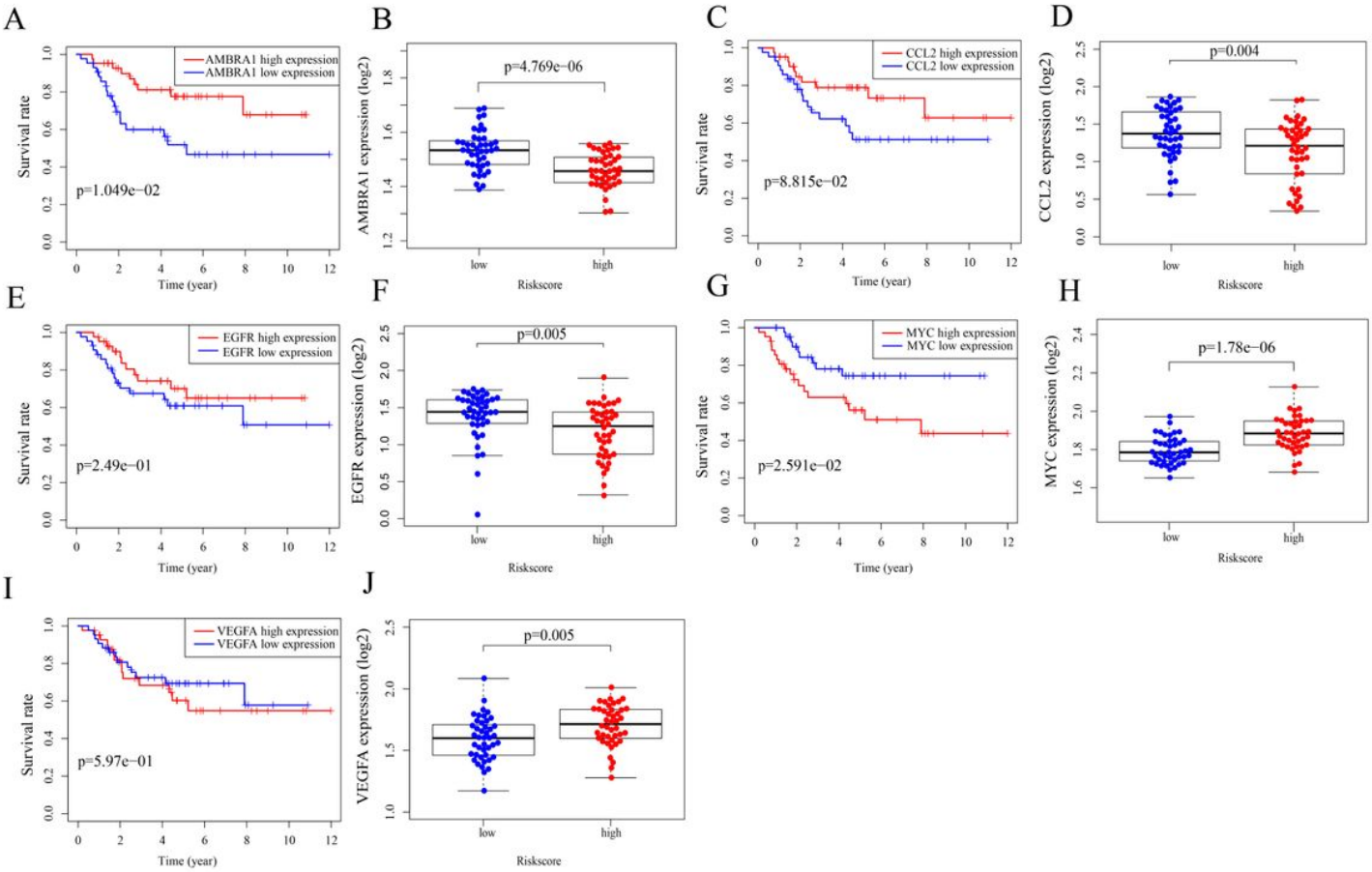

Figure 3

The survival rates and gene expressions of CCL2, AMBRA1, VEGFA, MYC and EGFR.

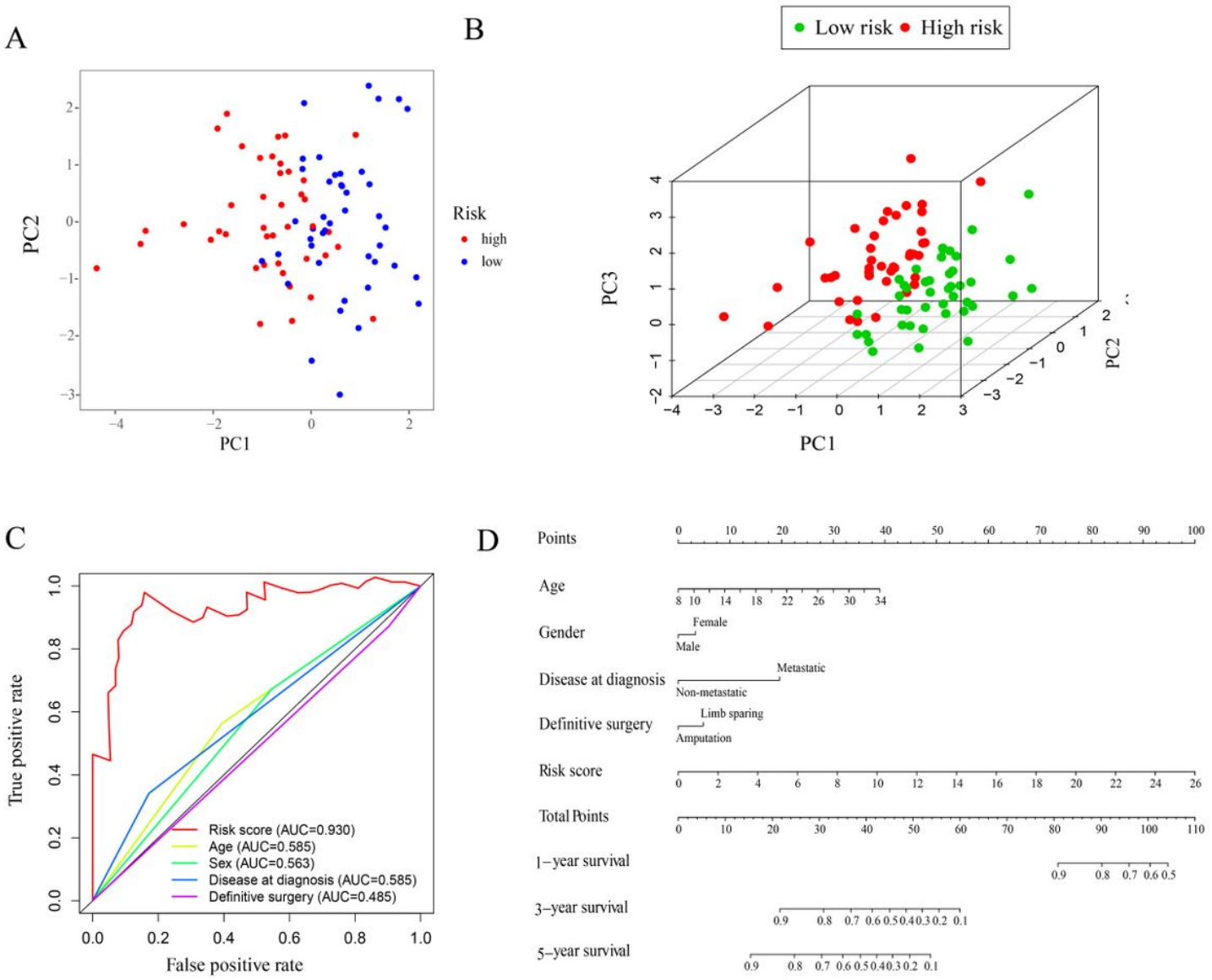

Figure 4

(A) Two-dimensional results of PCA. (B) Three-dimensional results of PCA. (C) Independent related risk factors (gender, age, disease at diagnosis, definitive surgery and risk score) selected in nomogram. (D) Nomogram for predicting 1-, 3-, 5-year survival.

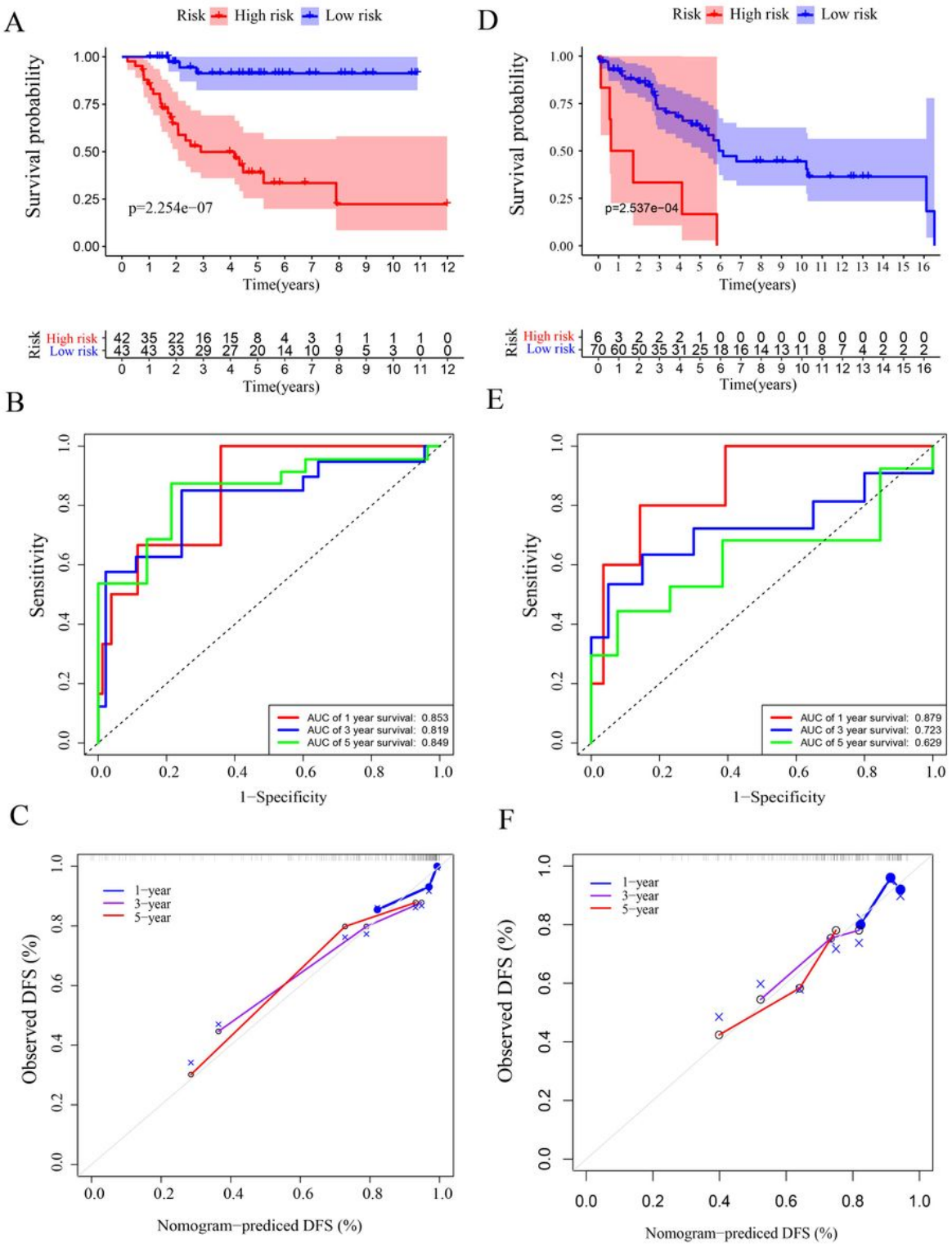

Figure 5

(A) Kaplan–Meier curve comparing the survival rates of high- and low-risk groups in training sets (B) ROC curve and (C) calibration curve to judge the accuracy of the nomogram in training sets. (D) Kaplan–Meier curve comparing the survival rates of high- and low-risk groups in validation sets (B) ROC curve and (C) calibration curve to judge the accuracy of the nomogram in validation sets.

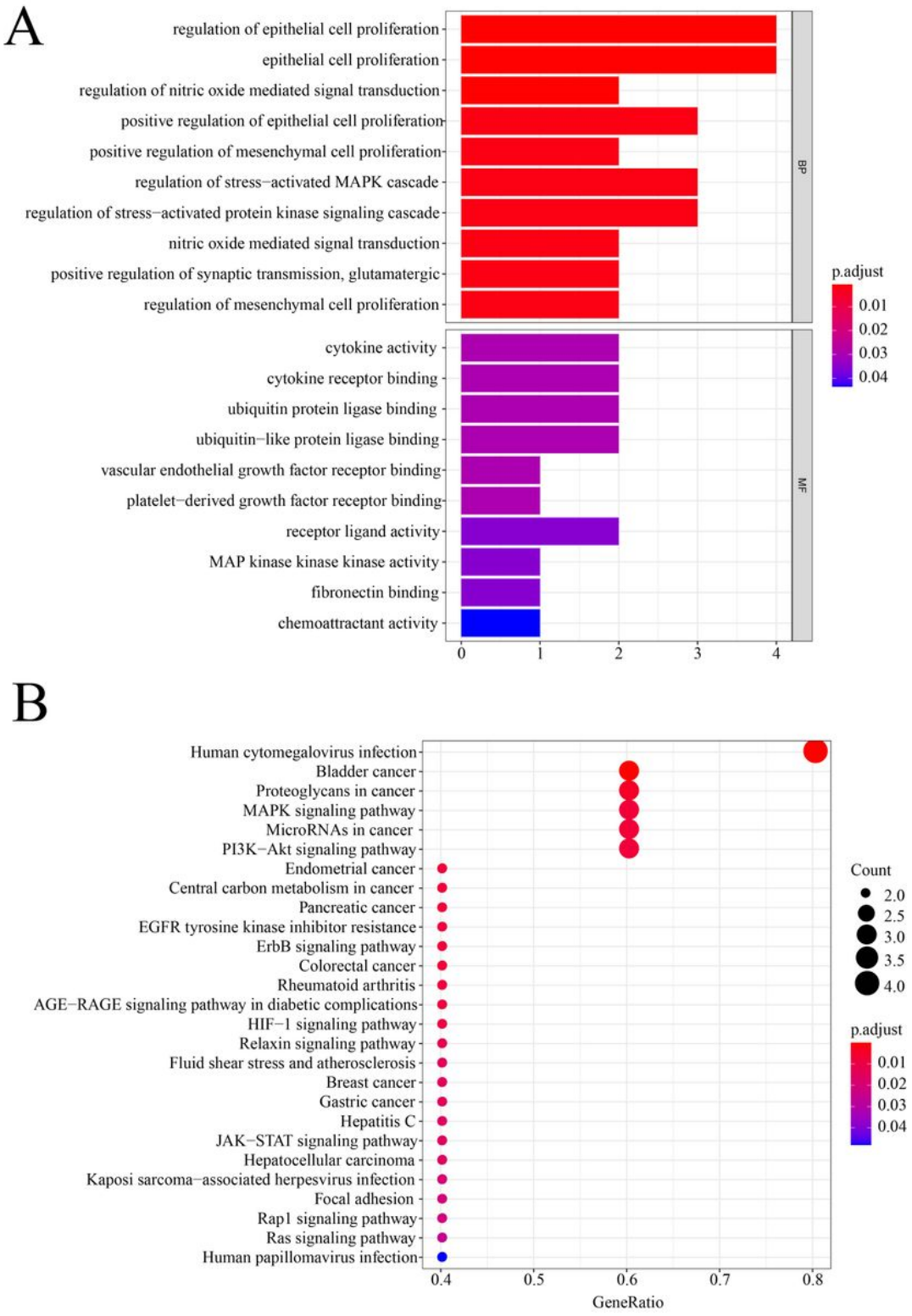

Figure 6

(A) Bar plot and (B) bubble plot of GO enrichment pathway. (C) Bar plot and (D) bubble plot of KEGG enrichment pathway.

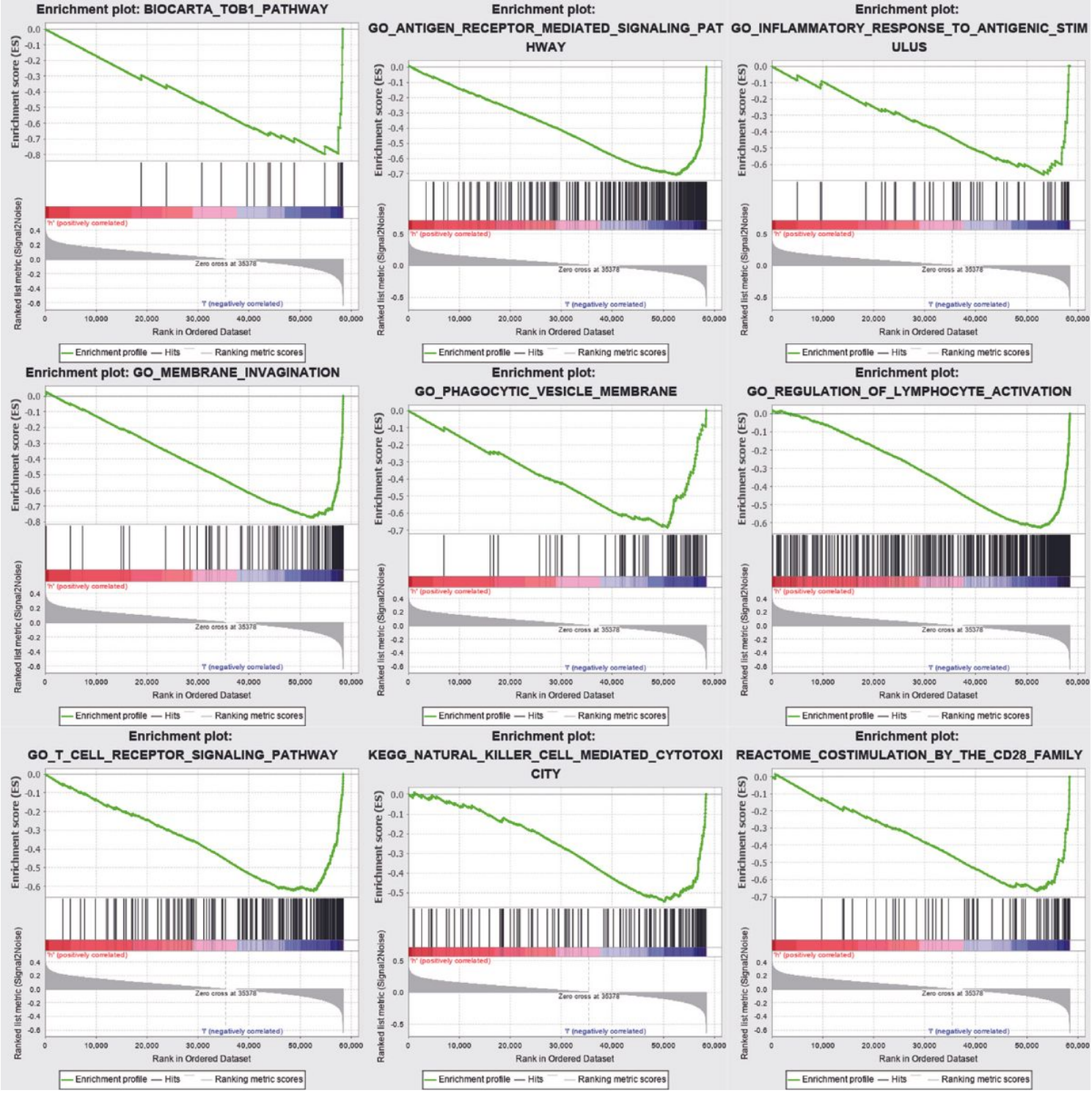

Figure 7

GSEA analysis results for CCL2, AMBRA1, VEGFA, MYC and EGFR.

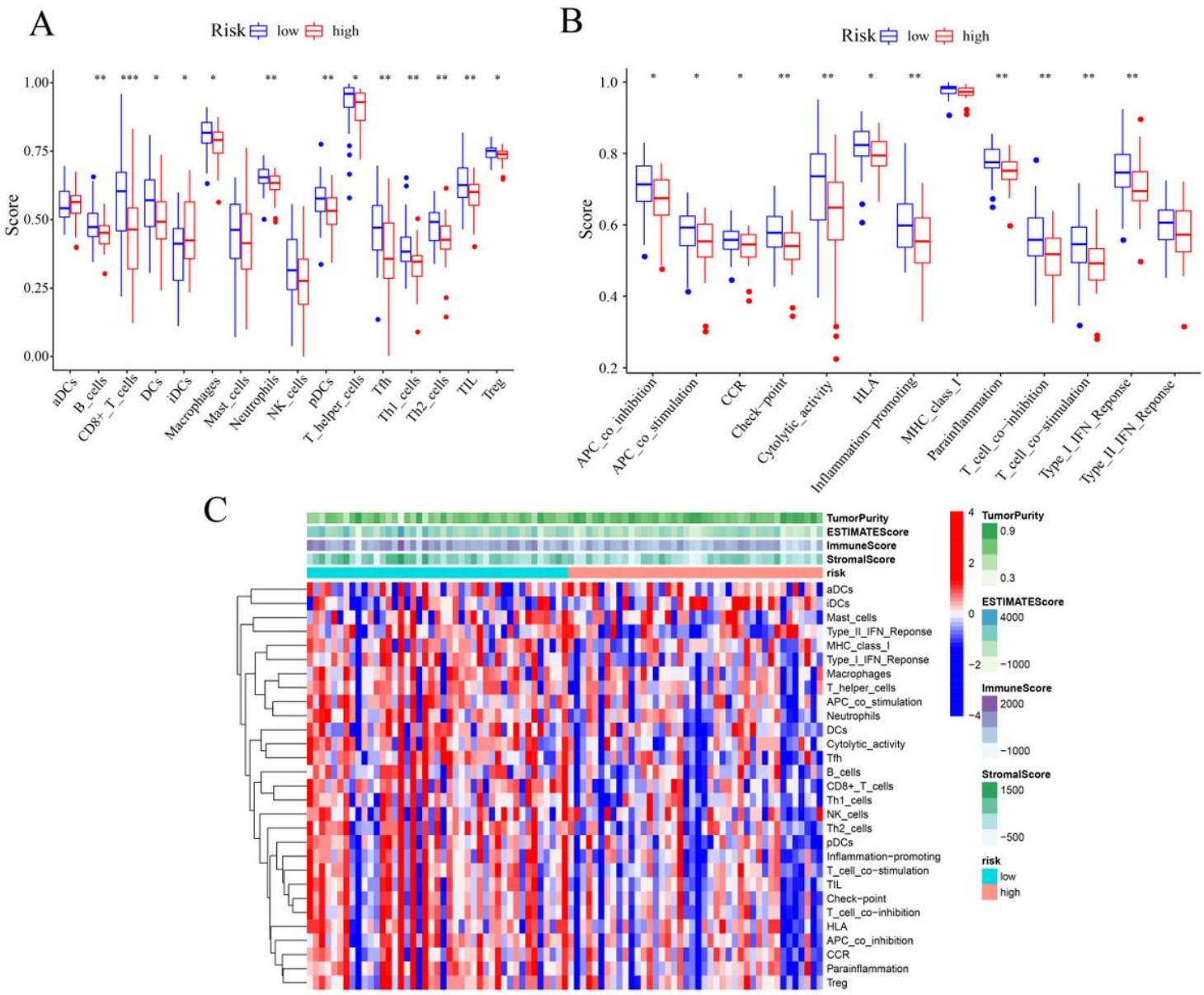

Figure 8

Tumor immune infiltration in low-and high-risk groups. (A) The 16 immune cell infiltration level in low-and high-risk groups. (B) The 13 immune function level in low-and high-risk groups. (C) Heatmap showing the infiltration level of immune cells in low-and high-risk groups.

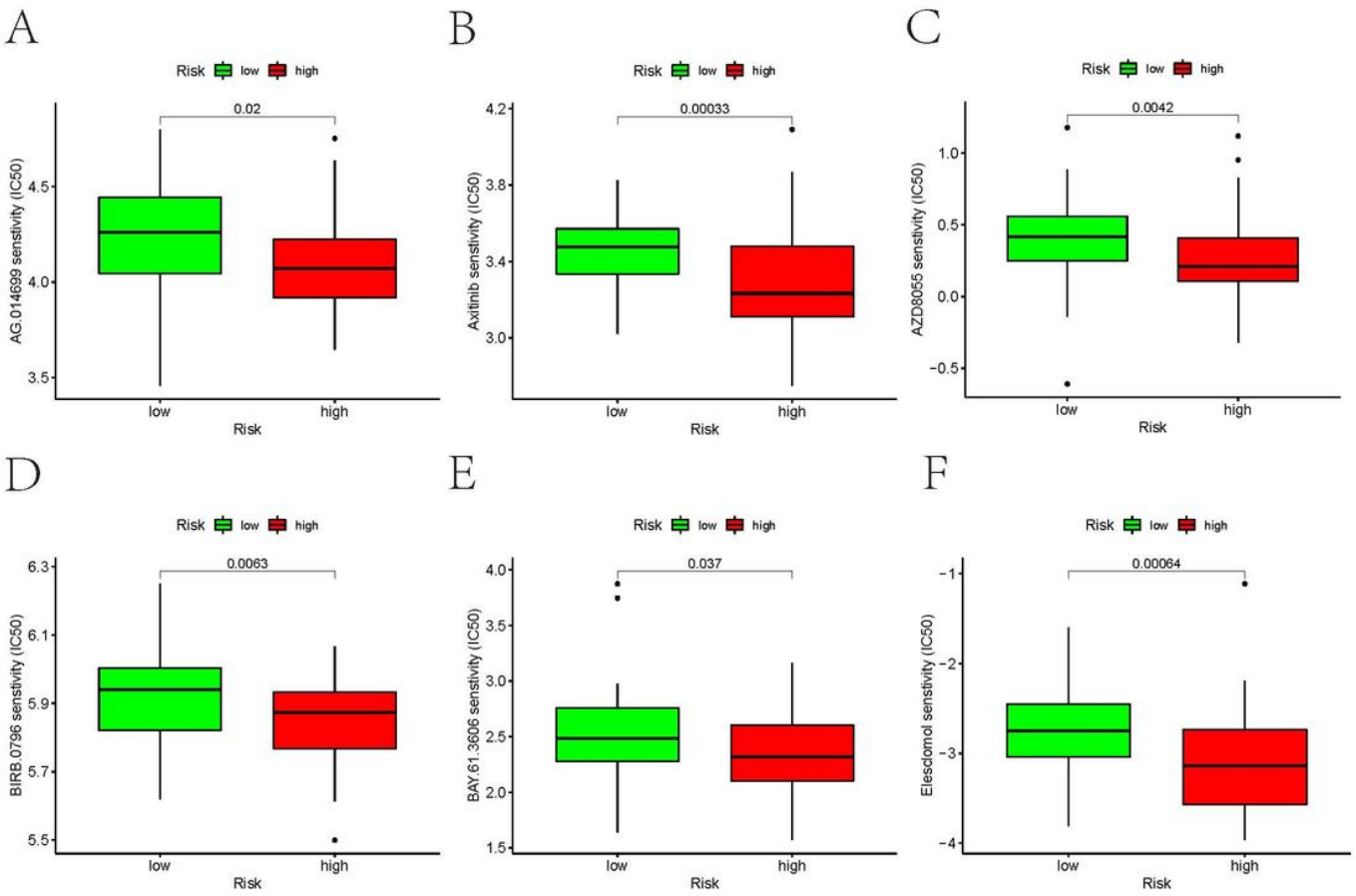

Figure 9

Prediction of response to targeted drugs. (A) AG.014699. (B) Axitinib. (C) AZD8055. (D) BIRB.0796. (E) BAY.61.3606. (F) Elesclomol.

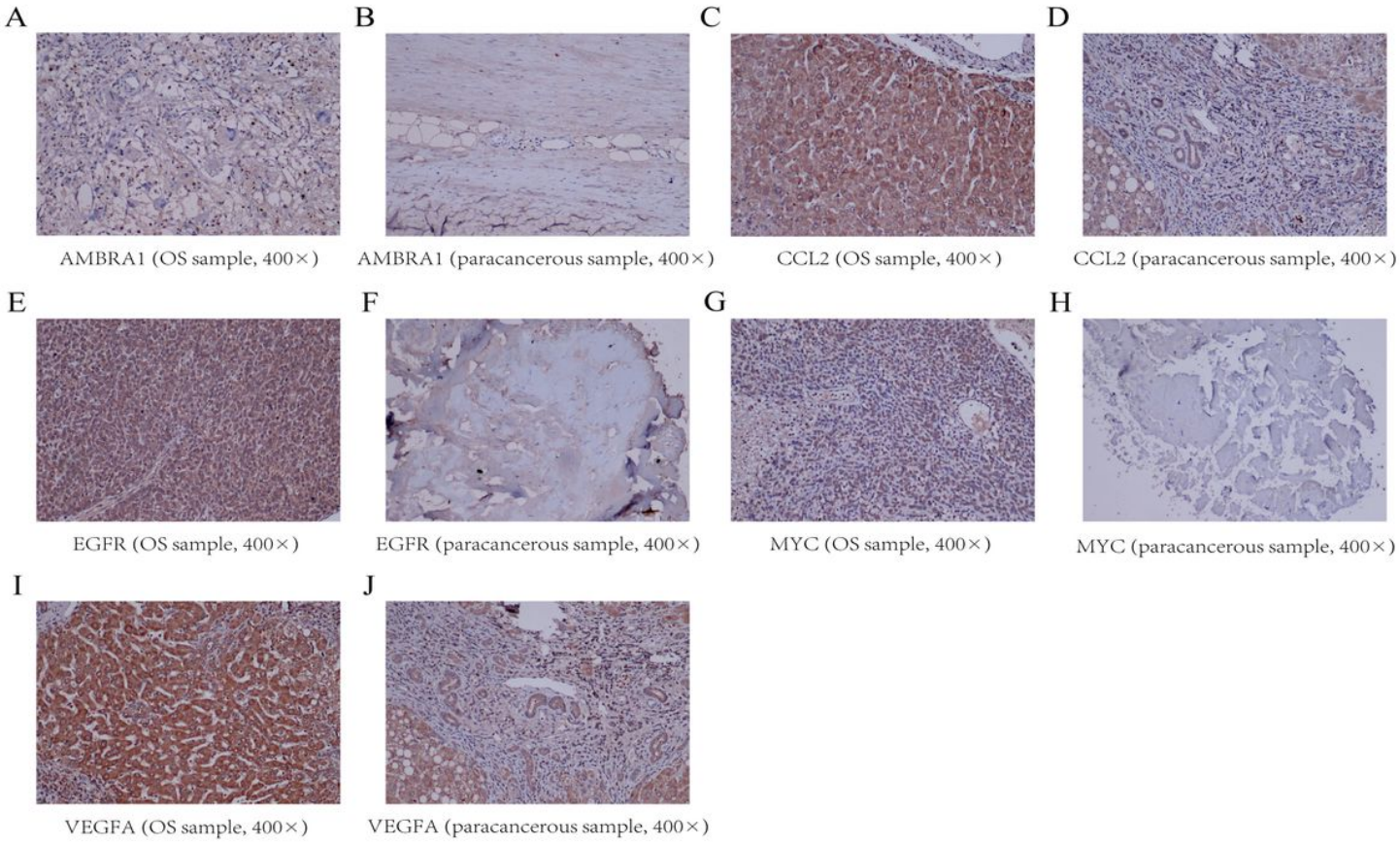

Figure 10

Immunohistochemistry result of CCL2, AMBRA1, VEGFA, MYC and EGFR.